146 11907 191707 348

Observations of Neutral Circulation at Mid-latitudes during the Equinox Transition Study

M. J. Buonsanto, ¹ J. E. Salah, ¹ K. L. Miller, ²

W. L. Oliver, 3 R. G. Burnside, 4 and P. G. Richards 5

Short title: Neutral Circulation during the Equinox Transition Study

(NASA-CR-184792) OBSIRVATIONS OF NEUTRAL CIRCULATION AT BIL-LATITUDES DUBING THE LOUINGX TRANSITION STUDY (Northeast Radio Observatory Corp.) 34 p CSCL 04A

N89-2 14 29

Uncla≨ c3/46 01917€7

- ¹ Haystack Observatory, Massachusetts Institute of Technology, Westford, Massachusetts
- ² Center for Atmospheric and Space Sciences, Utah State University, Logan, Utah
- ³ Department of Electrical, Computer, and Systems Engineering, Boston University, Boston, Massachusetts
 - ⁴ Arecibo Observatory, Arecibo, Puerto Rico
- ⁵ Center for Space Plasma and Aeronomic Research, University of Alabama in Huntsville, Huntsville, Alabama

Abstract

٥

Measurements of ion drift velocity made by the Millstone Hill incoherent scatter radar have been used to calculate the meridional neutral wind velocity during the Sept. 17-24, 1984 period. Strong daytime southward neutral surges were observed during the magnetically disturbed days of September 19 and 23, in contrast to the small daytime winds obtained as expected during the magnetically quiet days. The surge on September 19 was also seen at Arecibo. In addition, two approaches have been used to calculate the meridional wind component from the radar-derived height of the F-layer electron density peak. Results confirm the wind surge, particularly when the strong electric fields measured during the disturbed days are included in the calculations. The two approaches for the F-layer peak wind calculations are applied to the radar-derived electron density peak height as a function of latitude to study the variation of the southward daytime surges with latitude.

INTRODUCTION

Good progress has been made in the last decade in advancing our knowledge of the neutral thermospheric circulation. Experimentally, much new information has been obtained from satellite measurements (see Killeen and Roble [1988] for a review of Dynamics Explorer 2 results), incoherent scatter (IS) radars, Fabry-Perot (FP) interferometers, and more recently coordinated IS/FP measurements [eg. Burnside et al., 1983; Salah et al., 1987], and global campaigns [Oliver and Salah, 1988]. Satellite data has recently been used by Hedin et al. [1988] to create a global empirical wind model. A semi-empirical approach, which combines observations of the F2 peak height with MSIS neutral densities and temperatures and ionospheric models has also proven fruitful [Buonsanto, 1986; Miller et al., 1986; Forbes et al., 1988]. On the theoretical side, Thermospheric General Circulation Models (TGCM's) have been steadily improved, and several papers have documented

comparisons of these TGCM's with experimental data [eg., Hernandez and Roble, 1984; Forbes et al., 1987; Oliver and Salah, 1988, Crowley et al., this issue]. The latest TGCM's include tidal forcing at the lower boundary [Fesen et al., 1986] and auroral models with time-dependent parameterizations of auroral particle precipitation [Roble and Ridley, 1987]. The latest development is the self-consistent modeling of ionospheric and thermospheric processes [Rees et al., 1987; Roble et al., 1987b, 1988].

Studies of mid-latitude winds during quiet times reveal a general pattern of solar EUV-driven day-to-night circulation with zonally averaged winds directed from the summer to the winter hemisphere, and a seasonal transition which the NCAR TGCM predicted to occur abruptly near the equinoxes [Roble et al., 1977].

It was to investigate this transition period that the Equinox Transition Study (ETS), a global, coordinated, multi-instrument campaign, was organized and carried out during the period Sept. 17-24, 1984. This turned out to be an ideal period for detailed study on account of the variety of geomagnetic conditions which occurred. After a period of geomagnetic quiet, a small storm (Ap=36) occurred on September 19. Following a period of recovery, a major storm (Ap=112) occurred on September 23.

While the diurnally or zonally averaged global patterns of thermospheric neutral winds are becoming better understood, the diurnal and seasonal variations, particularly under varying geomagnetic conditions, are still poorly known. At high latitudes during storms, ion drag momentum forcing by the magnetospheric convection ionization drifts [eg., Killeen et al., 1984] is important in driving the neutral winds. The associated Joule heating and heating from particle precipitation results in post-midnight equatorward surges in the neutral wind, which have been modeled by the NCAR TGCM [Killeen and Roble, 1986; Roble et al., 1987a] and frequently observed at mid-latitudes [eg., Babcock and Evans, 1979; Murty and Kim,

1988]. Because optical measurements are limited to the night-time, there is less daytime data on neutral winds. However, Roble et al. [1978], and Hagan [1988] have
reported observations of day-time equatorward surges or propagating disturbances
in the meridional neutral wind during storms. Millstone Hill observations of an
equatorward day-time neutral surge on 19 September, 1984 have been already been
reported by Foster and Aarons [1988], and related to disturbance electric fields.
Theoretical models do not generally predict large scale changes in the day-time
meridional winds during storms at mid-latitudes, though Roble et al. [1987a]
reported an equatorward propagating disturbance during the daytime at midlatitudes in their simulations of the storm of March 22, 1979.

METHOD

The Millstone Hill (42.6°N, 288.5°E) incoherent scatter radar operated continuously through the ETS period, from 18:17 UT on Sept. 17 to 12:12 UT on Sept. 24, 1984. Both the fixed zenith-pointing 67 m antenna, and the fully-steerable 46 m antenna were used, each providing measurements of the electron densities, electron and ion temperatures, and plasma line-of-sight velocities. The steerable antenna was employed in making repetitive elevation scans to provide altitude/latitude cross-sectional maps of the ionospheric quantities. Two planes were used, one along the local meridian, and a second in a plane canted approximately 30° from the meridian. A pair of scans was completed in about 34 minutes. The zenithantenna measurements were interspersed with these scan measurements.

Using the line-of sight velocity data from the zenith-pointing position and two other appropriately selected positions, we are able to compute the full plasma velocity vector in the vicinity of Millstone Hill. Combining these with calculations the plasma diffusion velocity we obtain the "local" (above Millstone) neutral meridional wind at F region heights (see section 1 below). Because the elevation scans provided measurements over a wide latitude range of the peak height of the F₂

region electron density (hmF₂), as well as the electric field induced drift velocities (perpendicular to the magnetic field lines), it was possible to estimate the neutral winds using the techniques of Buonsanto [1986] and Miller et al. [1986] for the full latitude range of hmF₂ measurements (see sections 2 and 3 below). Thus the winds directly above Millstone Hill were obtained by three methods, and the consistency of the results gives more confidence in the latitude variation of the winds calculated by the latter two techniques.

In addition, incoherent scatter measurements of the neutral meridional wind above Arecibo (18.3°N, 293.2°E) will be presented, to show that the southward surges are seen at latitudes equatorward of the range of the Millstone Hill observations.

1. Neutral winds from incoherent scatter measurements of ion drift velocity

The technique used at Millstone Hill to derive the neutral wind component in the magnetic meridian from three-position ion drift radar measurements has been described in some detail by Oliver and Salah [1988], and it relies on the approach followed by Salah and Holt [1974] with some modifications. In brief, ion Doppler velocity measurements are required in three antenna positions; for the ETS campaign we used zenith, and 220° and 320° azimuths at an elevation of 40°. Measurements at these three positions, made at an altitude of 300 km, were then used to compute the ion drift velocity parallel to the magnetic field line over an average time interval of 34 minutes.

Subtraction of the ion diffusion velocity from the parallel ion drift yields the neutral wind component in the magnetic meridional direction, given by ($V\cos\delta + U\sin\delta$), where V is in the geographic northward direction, U is in the eastward direction, and δ is the magnetic declination (14°W) at Millstone Hill. The computation of the diffusion velocity depends on the basic plasma parameters (electron density and temperature and ion temperature) and their gradients in the F

region as determined from direct measurements by the radar. A key parameter in this computation, which affects the overall accuracy of the technique for night-time winds, is the ion-neutral diffusion coefficient which is discussed in section 4 below.

The overall statistical uncertainty in the neutral wind velocity determined by this technique is 20-30 m s⁻¹. At night, when diffusion effects are important, the accuracy of the technique depends on the knowledge of the neutral composition and the ion-neutral collision cross-section, primarily for O⁺-O collisions, and these result in an estimated overall wind accuracy of 50-70 m s⁻¹. While these accuracies apply during quiet and moderate geomagnetic conditions, during disturbed conditions we ascribe a larger uncertainty of 100 m s⁻¹ for the winds determined by this technique. This is due primarily to increased uncertainty in the neutral composition (particularly atomic oxygen).

2. Neutral winds from the Servo Model

The servo equations of Rishbeth et al. [1978] were first used by Buonsanto [1986] to calculate neutral winds. Minor modifications in the winds calculation were made in a subsequent paper [Buonsanto, 1988]. Because the present method is slightly different from that in earlier papers, it is briefly outlined here.

In the work done here equations (12) and (19) of Rishbeth et al. [1978] are used:

$$W = Hdz/dt + [e^{z} - e^{-kz}]D(\sin^{2}I)/2H$$
 (1)

where W is the vertical drift applied by a neutral wind or electric field,

$$k = 1.875$$

$$z = (hmF_2 - h_0)/H$$

where hmF2 is obtained from radar measurements

h_O is the balance height obtained from the level where the following are satisfied:

$$\beta = 0.628 \,\mathrm{D}(\sin^2 I)/\mathrm{H}^2$$
 (day) (2a)

$$\beta = 0.115 \, \text{D}(\sin^2 I)/H^2 \, \text{(night)} \, (2b)$$

with a gradual transition at sunrise and sunset based on the Chapman function. Here β is the recombination rate, obtained using MSIS-86 [Hedin, 1987] temperatures and densities. The Chen et al. [1978] reaction rate for $O^+ + O_2 \rightarrow O_2^+ + O$ is now used.

H = atomic oxygen scale height obtained from MSIS-86

I = magnetic dip angle

$$D = D_{in}(1 + T_e/T_i)$$

D_{in} = ion-neutral diffusion coefficient (see below)

 T_e and T_i are electron and ion temperatures obtained from IS radar measurements.

Then the poleward neutral wind is obtained from:

$$U_N = (v_{\perp N} \cos I - W)/(\cos I \sin I)$$
 (3)

where $v_{\perp N}$ is the ion drift velocity component perpendicular to the earth's magnetic field in the magnetic north direction, obtained from the IS radar.

Results will show that the effect of the dz/dt term in (1) is small so that to a good approximation:

$$W = [e^{z} - e^{-kz}]D(\sin^{2}I)/2H$$
 (4)

It may also be noted that the relation between W and z is non-linear. The effects of non-linearity are small except for strong drifts, as results below will show. For weak drifts (|z| small), (4) becomes:

$$W = z(k+1)D(\sin^2 I)/2H$$
 (5)

The accuracy of the servo model method for determining neutral winds depends primarily upon accuracy of the measurement of hmF₂ and of the neutral composition model and collision cross section. As will be shown below, the results are relatively insensitive to the adjustable parameters in the model (eg., the multiplicative factors in equation 2). The overall accuracy of the results should be

similar to those obtained from the line-of-sight velocities (section 1 above), provided that measured northward field-perpendicular velocities are included during disturbed periods.

3. Neutral winds from the method of Miller et al.

As mentioned above, results from servo model wind calculations will show that assuming a linear relationship between wind speed and the distance between hmF2 and the balance height does not normally result in statistically significant errors. Taking advantage of this approximate linearity, Miller et al. [1986] showed that the balance height and the constant of proportionality between meridional wind speed and layer height at a specified location, time, and solar conditions could be determined by modeling the F region at two wind speeds. The Field Line Interhemispheric Plasma (FLIP) Model was used to determine the height of the F region [Young et al., 1980; Richards and Torr, 1985]. Winds used in the modeling were pre-selected to bracket an average wind, thus minimizing the effect of the assumption of linearity.

The poleward neutral wind is obtained by equation (3), but in this case using $W = (hmF_2 - h_0)/\alpha$ (6)

where α is the calculated value of $\Delta hmF_2/\Delta W$ and h_0 is the calculated balance height. The derivation of meridional winds using the FLIP model is similar in many respects to the derivation using the servo model. Note the similarities of equations 5 and 6.

4. Ion-neutral diffusion coefficient

The O^+ ,O collision cross section was obtained from Dalgarno [1964]; Banks and Holzer [1968]. The O^+ ,N₂ and O^+ ,O₂ collision cross sections were obtained from Banks [1966]. Then:

$$D_{\rm in} = [kT_{\rm i}/m_{\rm O} +] \{1/[(\nu({\rm O}^+,{\rm O}) + \nu({\rm O}^+,{\rm N}_2) + \nu({\rm O}^+,{\rm O}_2)]\}$$

$$D_{in}=3.19x10^{19}T_{i}/\{f(T_{n}+T_{i})^{0.5}[O]+42.3[N_{2}]+41.1[O_{2}]\}$$
 (7)

Dalgarno [1964] gives f=1. However, a value of f=1.7 is suggested by recent work [Burnside et al., 1987]. Most of the results presented in this paper were obtained using f=1.7 in (7). f=1 is used in one instance to examine the sensitivity of the wind results to this factor.

RESULTS AND DISCUSSION

1. Neutral meridional winds above Millstone Hill

Figure 1 shows the neutral winds above Millstone Hill obtained from the IS line-of-sight velocity measurements, the servo model, and the method of Miller et al. [1986]. Note that 0 h local mean time corresponds to 4 h 46 m UT. It was found that slightly better agreement between the winds derived from the servo model and the winds derived from the IS velocity measurements was obtained when the empirical constant c in the servo equations, normally 1.33 for day, and 1.73 for night (for O₂ and N₂ loss equally important) was multiplied by a factor 0.75. This "tuning" of the servo model was included in the wind determinations shown in Figure 1. It results in the balance height being lowered to a height where:

$$\beta = 1.077D(\sin^2 I)/H^2$$
 (day) (8a)
 $\beta = 0.160D(\sin^2 I)/H^2$ (night) (8b)

Agreement between results shown in Figure 1 obtained with the three methods is generally good, although there is a small systematic offset of the IS line-of-sight velocity derived winds to more equatorward values and the Miller et al. winds to more poleward values with respect to the servo model winds. The IS line-of-sight velocity technique also gives a much larger equatorward surge near 12 UT on September 19. Some of the scatter in the servo and Miller et al. results is due to the limited altitude resolution of the IS hmF₂ measurements, and some is due to rapid variations in measured v_{LN} which are not reflected in the line-of-sight velocity derived winds.

The magnetic history switch in MSIS-86 was turned on for these calculations, i.e., an array of eight values, obtained from 3-hourly ap values for up to 59 hours before the current time, were input for each data point. This is necessary in order to utilize the capability of the MSIS-86 model to provide neutral composition and temperature values during periods with large changes in geomagnetic conditions (eg.

September 19 and 23). The effect on the IS and servo model results of turning on and off this ap history switch is shown in Figure 2. Use of the ap history generally results in stronger equatorward winds, especially at night, than those obtained using Daily Ap only.

The effect of tuning the servo model is shown in Figure 3 for one of the days of the period (September 21). The solid line shows winds calculated using equations 1,3, and 8, i.e., the tuned servo model, including non-linearity and the dz/dt term. The dotted line shows winds obtained using equations 1,2, and 3, i.e., the same as the solid curve, but using the standard servo model multiplicative factors. Generally the results are quite insensitive to the change in the multiplicative constants between (2a,b) and (8a,b). The tuning results in a maximum change of 29 m s⁻¹ in the calculated wind at 15 UT on September 21. Results are also shown in Figure 3 for the tuned servo model with the dz/dt term removed (winds obtained from equations 3,4, and 8), and for no dz/dt term and a linear relationship between W and z (winds obtained from equations 3,5 and 8). The results are close to those of the full, tuned servo model, with the largest difference on September 21 of 37 m s⁻¹ at 7 UT. Similar results were obtained on the other days of the ETS period. This shows the insensitivity of the results to both the dz/dt term and non-linear effects. Thus the Miller et al. method, which utilizes a formulation similar to equation 5, is not greatly affected in its ability to model the winds by its assumption of linearity.

The factor f, by which the O⁺,O collision cross section is multiplied, was set to 1.7 for the results given in Figure 1,2, and 3.

Miller et al. [1987] showed that for quiet or moderate geomagnetic conditions, the effect of electric fields on the neutral wind determination is generally small, and usually smaller than the statistical uncertainties in the calculation. The electric field correction, from (3), is given by $v_{\perp N}/\sin I$. It was obtained for the ETS period from IS measurements of the vector drift velocity, and the results are plotted in Figure 4.

Apart from a few data points on September 18, the magnitude of the correction $|v_{\perp N}/\sin I|$ is generally less than 30 m s⁻¹ on quiet days during the period. It is quite large on the disturbed days, however, reaching nearly 200 m s⁻¹ on September 19. This shows that during disturbed periods the effects of electric fields must be included in calculations of neutral winds obtained by an hmF₂ method.

Figure 5 gives the same results as Figure 1, except that the factor f in (7) was reduced to 1. For all three methods, this smaller O⁺,O collision cross section results in an increase in the magnitude of the calculated winds. The increase in the equatorward wind determined from the line-of-sight measurements is 105 m s⁻¹ at local midnight (5 UT) on September 18 and 60 m s⁻¹ for the day-time surge on September 19 at 12 UT. Such increases in the wind speed would also be produced by equivalent decreases in [O], or by some combination of decreases in [O], [N₂] and [O₂] from the MSIS-86 values. Thus, accurate determination of the O⁺,O cross section and the neutral concentrations is necessary for determination of the winds, either by incoherent scatter or by an hmF₂ technique.

Large-scale decreases in F region electron densities during storms are well known to be associated with decreases in the neutral atomic-to-molecular density ratio [eg., Prolss, 1987]. Unfortunately, the MSIS-86 neutral densities seem inconsistent with the observed ionospheric peak electron densities above Millstone Hill during the ETS period. Figure 6 shows observed day-time (10-16 LT) NmF₂ values together with values of the ratio $R = [O]/([N_2]+23[O_2])$, obtained from MSIS-86 for the peak heights hmF₂. This ratio was shown by Titheridge and Buonsanto [1983] to be proportional to the day-time equilibrium F region electron density. Although mean day-time NmF₂ drops from 4.2×10^{12} m⁻³ on September 18 to 2.6×10^{12} m⁻³ on September 19, (an apparent composition effect), mean R (at hmF₂) actually increases from 1.30 on September 18 to 1.47 on September 19. It should be noted that at a *fixed height* of 300 km, decreases in R do occur on the 19th,

but decreases do not occur if the time-varying hmF₂ values are input to MSIS. On September 23, R (at hmF₂) does decrease, but by a smaller percentage than NmF₂. Figure 7 shows the effects on the winds calculated by the servo model of an 80% increase on September 19 in [N₂] and [O₂], which would give R consistent with the 10-16 LT NmF₂ variation. The winds on the 19th become more poleward by ≈ 20 m s⁻¹. The value of the equatorward wind at 12 UT decreases from 198 m s⁻¹ to 180 m s⁻¹. Figure 7 also shows the effect on the servo model winds of an increase in [N₂] and [O₂] by a factor of 5. Richards et al. [1988] report that a decrease in [O]/[N₂] by a factor of 3 to 5 is needed by the field-aligned interhemispheric (FLIP) model of the ionosphere to explain the observed NmF₂ on September 19. A decrease in [O]/[N₂] by a factor of 5 reduces further the magnitude of the equatorward surges on September 19 calculated by the servo model and Miller et al. techniques, increasing the differences with the winds obtained from the IS line-of-sight velocity measurements. The maximum value of the equatorward surge given by the servo model method near 12 UT decreases from 198 m s⁻¹ to 136 m s⁻¹.

For the morning surge on September 19, Crowley et al. [this issue] reports that calculations using the Thermosphere/Ionosphere General Circulation Model (TIGCM) for Millstone Hill give an equatorward wind of approximately six hours duration with maximum value at 12 UT (7 LT) of 135 m s⁻¹. The IS winds derived from line-of-sight velocities are equatorward throughout the day time, however, and much larger in magnitude (maximum value 439 m s⁻¹ near 12 UT using f=1.7). This suggests that the changes to MSIS-86 required for consistency with the NmF₂ variations will include increases in [N₂] and [O₂], rather than decreases in [O], as increases in the densities would result in smaller equatorward winds consistent with the TIGCM. However a factor of 5 increase in [O₂] and [N₂] from the MSIS-86 values, with [O] held constant, only results in a decrease from 439 m s⁻¹ to 420 m s⁻¹ in the wind determined from the line-of-sight velocities near 12 UT on September 19.

This is because the MSIS O density is much larger than the MSIS N_2 and O_2 densities. Thus, the servo model maximum equatorward wind during the surge agrees with the TIGCM result if the $[O_2]$ and $[N_2]$ MSIS are increased by a factor of 5. However, the wind determined from the line-of-sight velocities is still higher than the TIGCM wind by a factor of about 4.

The strong southward surges in the daytime found on September 19 and 23 may be compared to the northward or weak southward winds in the daytime on the adjoining quiet days. The quiet-time behavior is consistent with previous such observations at mid-latitudes [eg. Vasseur, 1969; Salah et al. 1974]. On both September 19 and 23 the magnetic storm induced reversals and intensifications of the wind velocity were observed near 12 UT (7 LT). Foster and Aarons [1988] have already presented Millstone Hill observations of the day-time wind surge on September 19, and showed its relationship with disturbance electric fields which penetrated to low mid-latitudes during the event. A daytime surge has also been observed at Millstone Hill near 16 UT during the extremely disturbed (Ap = 202) conditions on February 8, 1986 [Hagan, 1988]. Roble et al. [1978] reported observations of a day-time equatorward propagating disturbance of about three hours duration following a sudden storm commencement on Sept. 18, 1974. A similar surge was found by Roble et al. [1987a] in their simulations of the storm of March 22, 1979. Thus it appears that the occurrence of day-time equatorward surges in the meridional neutral wind during storms may be a consistent feature of thermospheric dynamics.

2. Neutral meridional winds above Arecibo

Figure 8 shows the meridional winds at Arecibo obtained from the incoherent scatter radar there, plotted together with the Millstone Hill IS line-of-sight velocity derived wind results also shown in Figure 1. The equatorward surges on 19

September are seen at Arecibo (18.30N), though they are smaller in magnitude than

at Millstone. The maximum day-time equatorward wind of 439 m s⁻¹ at Millstone occurs at 1150 UT (7 LT), while at Arecibo the maximum wind occurs at 13 UT (9 LT) and is 171 m s⁻¹. Thus it takes about 70 minutes for the surge to travel from Millstone to Arecibo, implying a speed of propagation of about 550 m s⁻¹. This result is in excellent agreement with the speed of propagation of the gravity wave observed by Roble et al. [1978], which traveled from Millstone to Arecibo in about 75 minutes.

3. Latitude variation of the neutral meridional winds

Figure 9 shows the latitude variation of the meridional winds at the longitude of Millstone Hill throughout the ETS period using the servo model method for the latitude range 320 to 550 N geodetic latitude. Figure 10 gives corresponding results obtained from the FLIP model (Miller et al. method). To obtain both sets of results, hmF_2 was obtained from the IS radar, a factor f=1.7 was used in (7), the MSIS-86 densities were used with the ap history input and the measured $v_{\perp N}$ drift velocity values were included. In general, the latitude variation of the winds obtained by the two methods agree well. This gives more confidence in the two hmF2 wind calculation methods. The servo model winds, however, are systematically more negative (equatorward) by about 50 m s⁻¹. Tuning at most accounts for about half of this difference. Apart from this small systematic difference, our discussion of the ... magnitude of the daytime surge on September 19 leads us to believe that the uncertainties in the results shown in Figures 9 and 10 arise mainly from the model inputs (MSIS-86, hmF₂, collision cross section) rather than in the techniques themselves. Though the two methods are essentially equivalent, the servo model does have the advantage of simplicity and ease of calculation, relying as it does on analytical descriptions of the F2 peak. By contrast, the Miller et al. method has the advantage of a comprehensive field line interhemispheric model.

The equatorward surge near 12 UT on September 19 is shown by Figures 9 and 10 to cover the whole range of latitudes visible from Millstone. Strong post-

midnight surges are observed on September 19 and 23. On September 23 the daytime winds are initially equatorward, but turn poleward later in the day. During the quieter days (September 18, 20, 21, and 22, the normal pattern of equatorward nighttime winds and small day-time winds is evident.

Further work on day-time neutral surges, as discussed in this paper, should prove fruitful. The energy sources responsible for initiating the surges, i.e., Joule heating due to magnetospheric convection induced momentum forcing, as well as heating due to particle precipitation, need to be better quantified experimentally. This will improve inputs to the self-consistent thermosphere-ionosphere global models. For more accurate determination of the meridional winds from line-of-sight velocity or hmF2 measurements, the O+,O collision cross section and the neutral composition and temperature need to be better determined. An improved collision cross section can be obtained from laboratory measurements, quantum mechanical calculations, and from comparison of IS and Fabry Perot night-time results during quiet times, when the MSIS concentrations are more reliable. Independent measurements of neutral densities and temperatures during storms would be helpful to assess the validity of MSIS-86 under these conditions.

CONCLUSIONS

The results of this study of the meridional neutral wind observed from the Millstone Hill and Arecibo IS radars during the ETS period reveal the normal pattern of night-time equatorward winds and small day-time winds on the quiet days. On the magnetically disturbed days, strong equatorward surges are evident, with daytime (morning) surges on September 19 and 23. The magnitudes of the surges are still uncertain, due to the poorly known O⁺,O collision cross section and neutral composition. Further work on refining the collision cross section and better neutral composition and temperature estimates would help to resolve the apparent disagreement in the magnitude of the day-time surge on September 19 between the IS line-of-sight velocity measured winds and TIGCM results. This disagreement is only slightly reduced when increases (implied by the ionospheric behavior) in molecular nitrogen and oxygen densities above those given by MSIS-86 are used in the calculation of the diffusion velocity. The two methods [Buonsanto, 1986; Miller et al. 1986] for obtaining the latitude variation of the wind from the IS measured hmF₂ values have been shown to be essentially equivalent. These methods enabled determination of the meridional winds, including the southward surges, over a latitude range from 320 to 550 N geodetic latitude.

ACKNOWLEDGMENTS

We are grateful to D. G. Torr of the University of Alabama in Huntsville for contributions to the FLIP ionospheric model. We would like to thank Horng-Yu Wu at Utah State for preparation of contour plots. At Millstone Hill, thanks are due to R. Musgrove for calculations of the electric fields, to S. Cariglia for help with the IS wind calculations, and to John Foster, John Holt, and Maura Hagan for their help and useful discussions. Millstone Hill data were acquired and analyzed under the support of NSF cooperative agreement ATM-88-08137 to Massachusetts Institute of Technology. Support for K. L. Miller was provided by NSF Grant ATM-87-15367, and support for P. G. Richards by Grant ATM-87-16036. Arecibo Observatory is part of the National Astronomy and Ionosphere Center, operated by Cornell University under a cooperative agreement with the National Science Foundation.

REFERENCES

- Babcock, R. R., and J. V. Evans, Effects of geomagnetic disturbances on neutral winds and temperatures in the thermosphere observed over Millstone Hill, J. Geophys. Res., 84, 5349-5354, 1979.
- Banks, P. M., Collision frequencies and energy transfer, Ions, *Planet. Space. Sci., 14,* 1105-1122, 1966.
- Banks, P. M., and T. E. Holzer, Charge exchange and ion diffusion for thermal nonequilibrium conditions, *Planet. Space Sci.*, 16, 1019-1022, 1968.
- Buonsanto, M. J., Seasonal variations of day-time ionisation flows inferred from a comparison of calculated and observed NmF₂, J. Atmos. Terr. Phys., 48, 365-373, 1986.
- Buonsanto, M. J., Subsidiary maxima in late evening NmF_2 at a low latitude station at solar maximum, J. Atmos. Terr. Phys., 50, 573-578, 1988.

- Burnside, R. G., R. A. Behnke, and J. C. G. Walker, Meridional neutral winds in the thermosphere at Arecibo: Simultaneous incoherent scatter and airglow observations, J. Geophys. Res., 88, 3181-3189, 1983.
- Burnside, R. G., C. A. Tepley, and V. B. Wickwar, The O⁺-O collision cross-section: Can it be inferred from aeronomical measurements?, *Ann. Geophys.*, 5A, 343-350, 1987.
- Chen, A., R. Johnsen, and M. A. Biondi, Measurements of the $O^+ + N_2$ and $O^+ + O_2$ reaction rates from 300 to 900 K, J. Chem. Phys., 69, 2688-2691, 1978.
- Dalgarno, A., Ambipolar diffusion in the F region, J. Atmos. Terr. Phys., 26, 939, 1964.
- Fesen C. G., R. E. Dickinson, and R. G. Roble, Simulation of the thermospheric tides at equinox with the National Center for Atmospheric Research thermospheric general circulation model, J. Geophys. Res., 91, 4471-4489, 1986.
- Forbes, J. M., R. G. Roble, and F. A. Marcos, Thermospheric dynamics during the March 22, 1979, magnetic storm 2. Comparisons of model predictions with observations, J. Geophys. Res., 92, 6069-6081, 1987.
- Forbes, J. M., M. Codrescu, and T. J. Hall, On the utilization of ionosonde data to analyze the latitudinal penetration of ionospheric storm effects, *Geophys. Res. Lett.*, 15, 249-252, 1988.
- Foster, J. C., and J. Aarons, Enhanced antisunward convection and F region scintillations at mid-latitudes during storm onset, J. Geophys. Res., 93, 11537-11542, 1988.
- Hagan, M. E., Effects of geomagnetic activity in the winter thermosphere 2. Magnetically disturbed conditions, J. Geophys. Res., 93, 9937-9944, 1988.
- Hedin, A. E., MSIS-86 thermospheric model, J. Geophys. Res., 92, 4649-4662, 1987.
- Hedin, A. E., N. W. Spencer, and T. L. Killeen, Empirical global model of upper thermosphere winds based on Atmosphere and Dynamics Explorer Satellite data, J. Geophys. Res., 93, 9959-9978, 1988.

- Hernandez, G., and R. G. Roble, Nighttime variation of themospheric winds and temperatures over Fritz Peak Observatory during the geomagnetic storm of March 2, 1983, J. Geophys. Res., 89, 9049-9056, 1984.
- Killeen, T. L., and R. G. Roble, An analysis of the high-latitude thermospheric wind pattern calculated by a thermospheric general circulation model 2. Neutral parcel transport, J. Geophys. Res., 91, 11291-11307, 1986.
- Killeen, T. L., and R. G. Roble, Thermospheric Dynamics: Contributions from the first 5 years of the Dynamics Explorer Program, Rev. Geophys., 26, 329-367, 1988.
- Killeen, T. L., R. W. Smith, P. B. Hays, N. W. Spencer, L. E. Wharton, and F. G. McCormac, Neutral winds in the high latitude winter F region: Coordinated observations from ground and space, *Geophys. Res. Lett.*, 11, 311-314, 1984.
- Miller, K. L., D. G. Torr, and P. G. Richards, Meridional winds in the thermosphere derived from measurement of F_2 layer height, J. Geophys. Res., 91, 4531-4535, 1986.
- Miller, K. L., J. E. Salah, and D. G. Torr, The effect of electric field on measurements of meridional neutral winds in the thermosphere, *Ann. Geophys.*, 5A, 337-342, 1987.
- Murty, G. S. N., and J. S. Kim, Thermospheric temperatures and meridional winds measured at Albany, New York during geomagnetically disturbed periods, *Planet.*Space Sci., 36, 677-685, 1988.
- Oliver, W. L., and J. E. Salah, The global thermospheric mapping study, J. Geophys. Res., 93, 4039-4059, 1988.
- Prolss, G. W., Storm-induced changes in the thermospheric composition at middle latitudes, *Planet. Space. Sci.*, 35, 807-811, 1987.
- Rees, D., T. J. Fuller-Rowell, S. Quegan, R. J. Moffett, and G. J. Bailey,

 Thermospheric dynamics: Understanding the unusual disturbances by means of

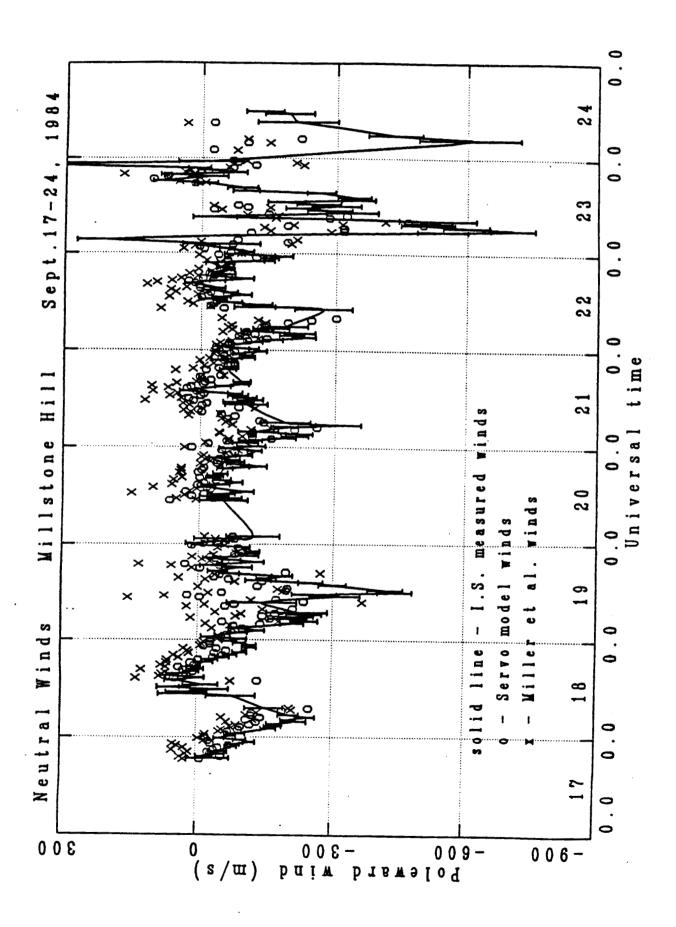
- simulations with a fully-coupled global thermosphere/high latitude ionosphere model, Ann. Geophys., 5A, 303-328, 1987.
- Richards, P. G., M. J. Buonsanto, D. G. Torr, and K. L. Miller, Magnetic storm effects on the ionosphere (abstract), EOS, Trans., AGU, 69, 1345, 1988.
- Richards, P. G., and D. G. Torr, Seasonal, diurnal and solar cycle variations of the limiting H⁺ flux in the earth's topside ionosphere, J. Geophys. Res., 90, 5261-5268, 1985.
- Rishbeth, H., S. Ganguly, and J. C. G. Walker, Field-aligned and field-perpendicular velocities in the ionospheric F2-layer, J. Atmos. Terr. Phys., 40, 767-784, 1978.
- Roble, R. G., and E. C. Ridley, An auroral model for the NCAR thermospheric general circulation model (TGCM), Ann. Geophys., 5A, 369-382, 1987.
- Roble, R. G., R. E. Dickinson, and E. C. Ridley, Seasonal and solar cycle variations of the zonal mean circulation in the thermosphere, J. Geophys. Res., 82, 5493-5504, 1977.
- Roble, R. G., A. D. Richmond, W. L. Oliver, and R. M. Harper, Ionospheric effects of the gravity wave launched by the September 18, 1974 sudden commencement, *J. Geophys. Res.*, 83, 999-1009, 1978.
- Roble, R. G., J. M. Forbes, and F. A. Marcos, Thermospheric dynamics during the March 22, 1979, magnetic storm 1. Model simulations, J. Geophys. Res., 92, 6045-6068, 1987a.
- Roble, R. G., E. C. Ridley, and R. E. Dickinson, On the global mean structure of the thermosphere, J. Geophys. Res., 92, 8745-8758, 1987b.
- Roble, R. G., E. C. Ridley, A. D. Richmond, and R. E. Dickinson, A coupled thermosphere/ionosphere general circulation model, *Geophys. Res. Lett.*, 15, 1325-1328, 1988.
- Salah, J. E., and J. M. Holt, Midlatitude thermospheric winds from incoherent scatter radar and theory, *Radio Sci.*, 9, 301-313, 1974.

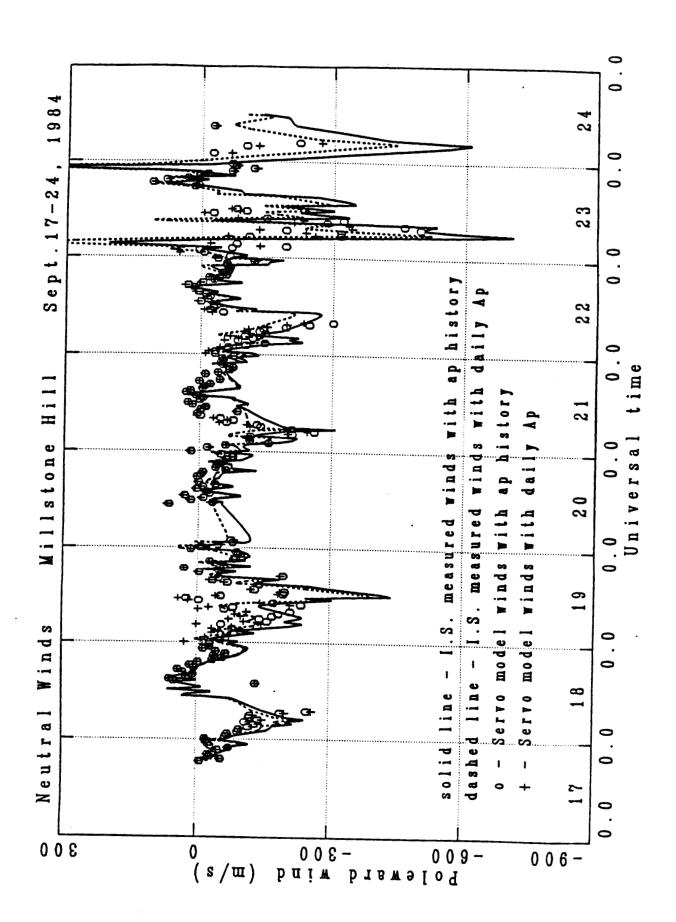
- Salah, J. E., J. V. Evans, and R. H. Wand, Seasonal variations in the thermosphere above Millstone Hill, Radio Sci., 9, 231-238, 1974.
- Salah, J. E., G. Hernandez, R. G. Roble, and B. A. Emery, Longitudinal and latitudinal dependencies of thermospheric winds from incoherent scatter radar and optical emission Doppler shift measurements, *Ann. Geophys.*, 5A, 359-362, 1987.
- Titheridge, J. E., and M. J. Buonsanto, Annual variations in the electron content and height of the F layer in the northern and southern hemispheres, related to neutral composition, J. Atmos. Terr. Phys., 45, 683-696, 1983.
- Vasseur, G., Vents dans la thermosphere deduits des mesures par diffusion de Thomson, Ann. Geophys., 25, 517-524, 1969.
- Young, E. R., D. G. Torr, P. G. Richards, and A. F. Nagy, A computer simulation of the midlatitude plasmasphere and ionosphere, *Planet. Space Sci.*, 28, 881-893, 1980.
- M. J. Buonsanto and J. E. Salah, MIT Haystack Observatory, Westford, MA 01886.
 - R. G. Burnside, Arecibo Observatory, P. O. Box 995, Arecibo, Puerto Rico 00613.
- K. L. Miller, Center for Atmospheric and Space Sciences, Utah State University, UMC 34, Logan, UT 84322.
- W. L. Oliver, Department of Electrical, Computer, and Systems Engineering, Boston University, Boston, MA 02215.
- P. G. Richards, Center for Space Plasma and Aeronomic Research, University of Alabama in Huntsville, Huntsville, AL 35899.

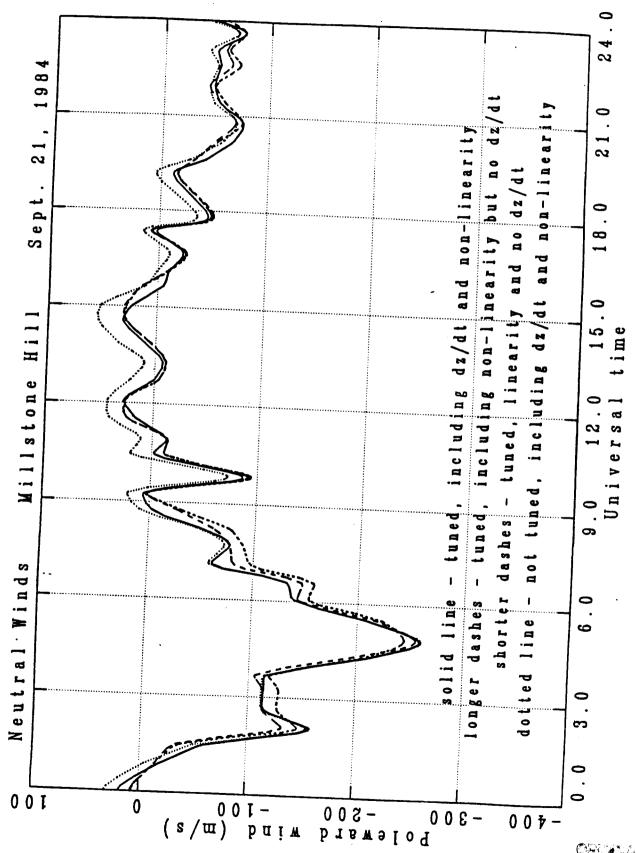
Figure Captions

- Fig. 1. Neutral meridional winds in the thermosphere above Millstone Hill during the ETS period. In all calculations the ap history was input to the MSIS-86 model, and f = 1.7 was used in the calculation of the ion-neutral diffusion coefficient. Solid line: winds at 300 km from IS line-of-sight velocity measurements. Circles: winds at hmF2 from the Servo model. Crosses: winds at hmF2 from the FLIP model (Miller et al.) method. 0 h local mean time corresponds to 4 h 46 m UT.
- Fig. 2. Winds obtained from IS line-of-sight velocity measurements and from the servo model, showing the effect of turning on and off the ap history switch in MSIS-86.
- Fig. 3. Servo model winds on Sept. 21, 1984, showing the effects of the dz/dt term, non-linearity, and tuning.
- Fig. 4. The electric field correction to the servo model and Miller et al. winds above Millstone Hill, obtained from IS measurements of the magnetic field perpendicular north-south ion velocity.
- Fig. 5. Same as Fig. 1., except using f = 1 in the calculation of the ion-neutral diffusion coefficient.
- Fig. 6. Observed daytime (10 16 local time) NmF₂ obtained from the Millstone Hill Digisonde, and the atomic to molecular density ratio R (see text) obtained at the measured peak height hmF₂ from the MSIS-86 model.
- Fig. 7. Servo model winds on September 18 and 19, showing the effect of increasing the MSIS-86 N_2 and O_2 densities.
- Fig. 8. Neutral winds obtained from IS line-of-sight velocity measurements at Arecibo, compared with those above Millstone Hill.
- Fig. 9. Latitude variation of the meridional neutral winds (m s⁻¹) at the longitude of Millstone Hill, calculated using the servo model.

Fig. 10. Same as Fig. 9, but using the FLIP model (Miller et al. method) to calculate the meridional wind speed.







OFFICER CALLY

